

ON DETECTING THE X-RAY SILHOUETTE OF A DAMPED LYMAN α SYSTEM

MARK DIJKSTRA, ZOLTÁN HAIMAN & CALEB SCHARF

Department of Astronomy, Columbia University, 550 West 120th Street, New York, NY 10027

Submitted to ApJ

ABSTRACT

We explore the possibility of resolving an image of a damped Lyman α (DLA) system in absorption against an extended, diffuse background X-ray source. Typical columns of neutral hydrogen in DLAs are high enough to block out up to $\sim 30\%$ of the soft X-ray flux at an observed photon energy of 0.5 keV, and we find that $\sim 1\%$ of the area of extended X-ray sources at $z \gtrsim 1$ have their 0.5 keV flux reduced by at least 20%. We discuss the observability of such absorption and find that $\lesssim 2$ arcsecond resolution, and $\gtrsim 300$ photons per angular resolution element are required in the 0.3–8 keV band for its detection, and in order to distinguish it from intrinsic surface brightness fluctuations. For the surface brightness of the currently known high-redshift extended X-ray sources, this requires an integration time of a few Msec on *Chandra*. The detection will be within the reach of a routine observation with a next generation X-ray telescope such as *XEUS* or *Generation X*.

Subject headings: cosmology: theory – galaxies: formation – galaxies: high-redshift – quasars: absorption lines
– X-rays: galaxies

1. INTRODUCTION

Damped Lyman α (DLA) absorbers owe their name to the presence of broad damping wings in their absorption profiles caused by column densities of neutral hydrogen in the range $N_{\text{HI}} \sim 10^{20} - 5 \times 10^{21} \text{ cm}^{-2}$. These high column densities are only found in the cold disks of late-type galaxies in the local universe, but to identify the galaxies hosting this gas at cosmological redshifts has proven difficult, because of the overwhelming brightness of the background quasar in the optical. Only a dozen probable hosts for DLAs at $z \lesssim 1$ have been identified and their morphologies span a wide range (Chen & Lanzetta 2003; Rao et al. 2003).

So far several hundred DLAs have been found in optical and ultraviolet quasar absorption spectra in the redshift range $z \sim 0.1 - 4.6$ (Curran et al. 2002). It has been shown that at $z \gtrsim 3$ they are the main contributors to Ω_{HI} (Rao & Turnshek 2000; Storrie-Lombardi & Wolfe 2000; Prochaska & Herbert-Fort 2004), and make up the largest reservoir of cold gas available for starformation. Indeed, Ω_{HI} at $z \approx 3$ is comparable to Ω_* at $z \approx 0$, the cosmic mass density of stars in the local universe (Wolfe et al. 1995).

It has therefore been argued that DLAs are the progenitors of present-day galaxies. The exact nature of these progenitors however, is controversial: Some have argued that DLAs are large proto-galactic disks, based on (i) the asymmetric profiles of the low-ionization absorption lines, which are explained if the metals are present in a large, rapidly rotating disk (Prochaska & Wolfe 1997) and (ii) the large ($R > 15$ kpc, e.g. Chen & Lanzetta 2003) physical separation between the absorber and possible associated starlight in a few cases. Others have argued that these data are also consistent with DLAs being a collection of much smaller ($\lesssim 5$ kpc) compact HI clouds falling onto a galaxy in their vicinity (Haehnelt et al. 1998).

Determining the nature of the progenitors of our present day galaxies is an important step in understanding galaxy formation in general. Obtaining a spatially resolved image of the neutral gas in a DLA will be an important step in settling this issue. Unfortunately, detecting the neutral hydrogen in DLAs in emission at $z \gtrsim 0.5$ using the 21cm line on an existing telescope such as the Giant Meter-wave Radio Telescope (GMRT) is not feasible (e.g. Bagla 1999). Among planned future radio telescopes, only

the Square Kilometer Array (SKA) has the appropriate sensitivity and frequency range to make such observations.

A major hindrance for constraining the properties of the DLA gas is the point-like character of the background quasars. Finding DLAs in absorption against extended background sources would provide valuable additional information. In one example, Briggs et al. (1989) found that the dimensions of a disk-like absorber at $z = 2$ are > 11 kpc against a background extended radio source; ruling out compact gas configurations such as dwarf galaxies. In another case, Kanekar & Briggs (2003) have found HI 21cm absorption in a gravitational lens system at $z = 0.76$ towards a quasar, from which the column density of hydrogen in the lens was estimated to be $(2.6 \pm 0.3) \times 10^{21} \text{ cm}^{-2}$. The lens is therefore a DLA, but because the largest separation between a pair of radio images was small, ~ 0.7 arcsec, the physical extent of the absorber is not well constrained.

In this paper, we examine the complementary possibility of detecting DLAs against an extended background source emitting X-rays. The motivation for this approach is the discovery of the extended X-ray source 4C41.17 by Scharf et al. (2003) at $z = 3.8$, with diffuse emission extending over ~ 100 arcsec². The X-ray spectrum is non-thermal and has a power-law index consistent with that of radio synchrotron emission. Scharf et al. (2003) conclude that the X-rays are most likely inverse Compton scattered cosmic microwave (CMB) or far infrared background photons. A very similar source, 3C294, was found by Fabian et al. (2003) at $z = 1.8$ with diffuse emission extending over ~ 200 arcsec².

A silhouette of a galaxy containing neutral hydrogen against a background X-ray cluster has already been found at low redshift ($z = 0.02$, Clarke et al. 2004) and encourages us to explore diffuse X-ray sources as possible background screens against which to image DLAs. Bechtold et al. (2001) found evidence for X-ray absorption in the spectrum of a $z = 1.1$ quasar, a point source, in the direction of a $z = 0.3$ DLA. Our calculations focus on an observed photon energy of $E = 0.5$ keV. This choice reflects the fact that the absorption signature is strongest in the range $E \sim 0.3 - 0.6$ keV (see §3), and that X-ray detectors are significantly less efficient at lower energies.

The outline of the rest of this paper is as follows: In §2, we calculate the covering factor of DLAs on the sky as a function of the fraction of soft X-ray photons they absorb. In §3, we describe how absorption by a DLA can be distinguished from intrinsic surface brightness fluctuations. In §4, we discuss several related issues, such as contamination of the absorption signature by a foreground object, model uncertainties, and the “inverse method” of searching for X-ray emission behind known DLAs. Finally, in §5, we present our conclusions and summarize the implications of this work.

2. SILHOUETTES OF DLAS

Typical neutral hydrogen column densities in DLAs are in the range $N_{\text{HI}} \sim 10^{20} - 5 \times 10^{21} \text{ cm}^{-2}$ and are large enough to block a non-negligible fraction of X-rays emitted by sources that lie behind them. The optical depth through a column N_{HI} of hydrogen atoms for a photon of energy E is $\tau(E) \sim 0.04 (N_{\text{HI}}/10^{21})(E/1 \text{ keV})^{-3.1}$, for a gas that consists solely of a cosmic mix of 76% neutral hydrogen and 24% helium by mass. Observations indicate that the mean metallicity of DLAs is ~ 0.1 times the solar value with a modest redshift evolution (Prochaska et al. 2003). The presence of metals increases the optical depth. For example, the cross section per hydrogen atom in a gas with metallicity $Z = 0.1Z_{\odot}$ is $\sim 1.4(E/1.0 \text{ keV})^{0.5}$ times larger than in a metal free gas (e.g. Wilms et al. 2000). This shows that DLAs can show up in absorption against bright background X-ray sources, something that has most likely been detected already by Bechtold et al. (2001), although in their case the background source was point-like.

The main question is therefore not whether DLAs can absorb some observable fraction of X-rays but what fraction of the sky is covered by these DLAs. More specifically, we quantify below what fraction of the sky is covered by DLAs, through which the optical depth is $\geq \tau_{0.5}$ at $E = 0.5 \text{ keV}$ in the observers frame as a function of $\tau_{0.5}$.

To calculate N_{HI} , the column of hydrogen atoms in the DLA, required to produce an optical depth $\geq \tau_{0.5}$, we need to know σ_{tot} , the total absorption cross-section per hydrogen atom. This cross-section should include absorption by helium and heavier elements. To calculate $\sigma_{\text{tot}}(E)$ of the DLA gas, we use the model described by Wilms et al. (2000). This model includes up-to-date photoionization cross sections and heavy elements in a solar abundance pattern, as well as H_2 molecules. An important uncertainty is the metallicity of the gas in the DLA, which can vary by an order of magnitude between individual objects (Prochaska et al. 2003). As a fiducial model we take $Z_{\text{DLA}} = 0.1Z_{\odot}$, consistent with the mean observed metallicity. We note that X-ray absorption arises predominantly from inner shells ionizations of metals, and ionization corrections are only important at gas temperatures much higher than expected to occur in DLAs.

Given $\sigma_{\text{tot}}(E)$ and requiring $N_{\text{HI},\text{min}}\sigma_{\text{tot}}(E = 0.5 \text{ keV}) = \tau_{0.5}$, we obtain a minimum column density of hydrogen $N_{\text{HI},\text{min}}$ for the DLAs, which changes as a function of redshift because of the redshifting of the photon energy (i.e. $\sigma_{\text{tot}}(E')$ is computed at $E' = E[1+z]$). In Figure 1, we show $N_{\text{HI},\text{min}}(z)$ as a function of redshift for the particular case $\tau_{0.5} = 0.1$. For any other value of $\tau_{0.5}$, the minimum column can be obtained by multiplying the value taken from Figure 1 by $\tau_{0.5}/0.1$. To illustrate the importance of the assumed metallicity, we show three cases: $Z = 0$ (blue-dashed), $Z = Z_{\odot}$ (red-dotted), and $Z = 0.1Z_{\odot}$ (black-solid). The last is our fiducial model. The reason N_{HI} drops

slightly but suddenly at $z \sim 0.4, 0.7, 1.6, \dots$ is that $E = 0.5(1+z) \text{ keV}$ at these redshifts equals the K-shell transition energy of one of the heavy elements.

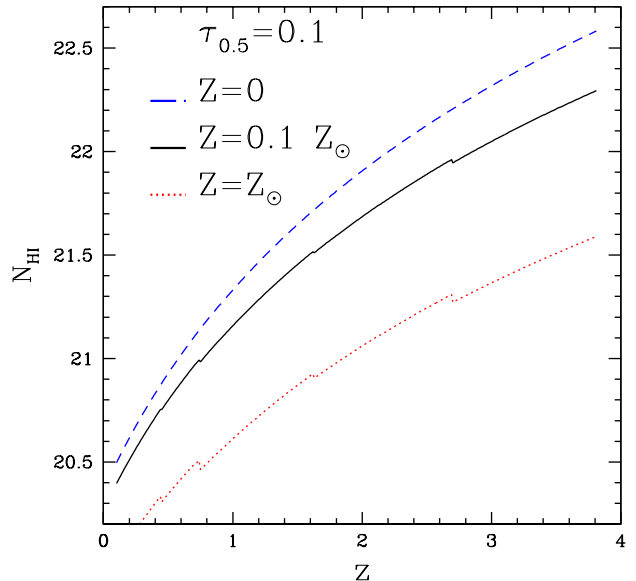


FIG. 1.— The column density of hydrogen required to produce an absorption optical depth of $\tau_{0.5} = 0.1$ for photons with observed energy $E = 0.5 \text{ keV}$, as a function of redshift for three metallicities. To illustrate the importance of metallicity in DLAs, we show three cases: DLAs with no metals (blue-dashed), with $Z = Z_{\odot}$ (red-dotted) and $Z = 0.1Z_{\odot}$ (black-solid). The last is our fiducial model. The highest column of hydrogen in a DLA that has been observed has $\log(N_{\text{HI}}) = 21.7$ (Curran et al. 2002).

The total number of DLAs along a single line of sight with column density exceeding $N_{\text{HI},\text{min}}$ between redshift 0 and z_s , where z_s is the redshift of a hypothetical extended background source, is given by:

$$\mathcal{N} = \int_0^{z_s} dz \int_{N_{\text{HI},\text{min}}(z)}^{\infty} dN_{\text{HI}} f(N_{\text{HI}}, z) \quad (1)$$

where $f(N_{\text{HI}}, z) dN_{\text{HI}} dz$ is the number of DLAs in the range $N_{\text{HI}} \pm dN_{\text{HI}}/2$ and $z \pm dz/2$. We adopt $f(N_{\text{HI}}, z)$ from Péroux et al. (2003; hereafter P03) who find that the data can be best fit with a Γ function used in studies of the galaxy luminosity function.¹ Note that \mathcal{N} can equivalently be interpreted as the 2-dimensional covering factor of these DLAs; $f_{\text{cov}} \equiv \mathcal{N}$. The exact form of $f(N_{\text{HI}}, z)$ is another important uncertainty in our model. The total sample of DLAs is still too small to constrain $f(N_{\text{HI}}, z)$ well, especially at low redshifts and high-column densities that are most important for our purposes. We discuss this uncertainty in more detail in §4.2.

In Figure 2, we plot f_{cov} as a function of $\tau_{0.5}$, with the X-ray source located at $z_s = 3.8$ (motivated by the source found by Scharf et al. 2003, 4C41.17). For example, this figure shows that a fraction $f_{\text{cov}} \sim 0.03/0.01$ is covered by DLAs that absorb at least $\sim 10/20\%$ of the 0.5 keV photons from the background object respectively. For different energies, $\tau_E \sim \tau_{0.5} \times [\sigma_{\text{tot}}(E)/\sigma_{\text{tot}}(0.5 \text{ keV})]$, since the absorption cross-section is

¹Note that we obtain $f(N_{\text{HI}}, z)$ by multiplying the functions quoted in P03 by $dX(z)/dz$. Their function describes the number of DLAs in the range $X(z) \pm dX(z)/2$, where $dX(z)/dz \equiv (1+z)^2 (H_0/H(z))$ is the absorption distance, originally introduced by Bahcall & Peebles (1969), where H_0 and $H(z)$ is the Hubble parameter at redshift 0 and z , respectively. We use the cosmological parameters $\Omega_m = 0.27$, $\Omega_{\Lambda} = 0.73$, and $h = 0.71$ presented by Spergel (2003).

close to a pure power-law.

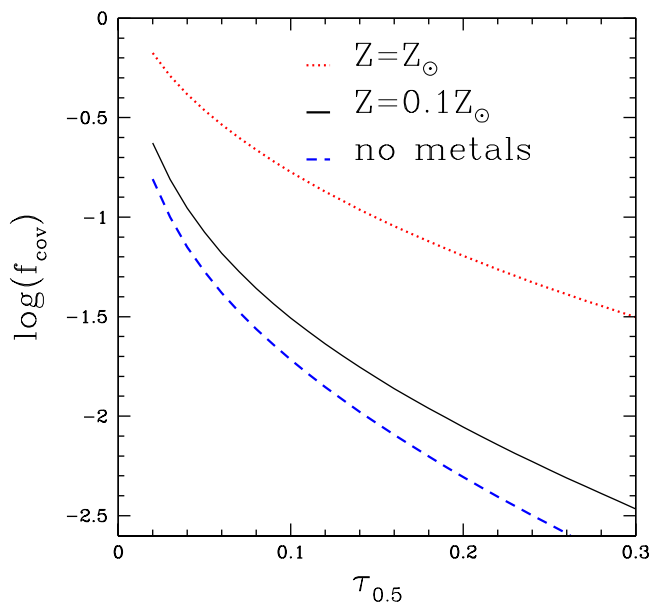


FIG. 2.— The covering factor f_{cov} on the sky of DLAs between $z = 0$ and $z_s = 3.8$ that are optically thicker than $\tau_{0.5}$ for a 0.5 keV photon in the observers frame, as a function of $\tau_{0.5}$. The three curves represent the same three metallicities as in Figure 1.

We examined in an alternative model the effect of the observed scatter in metallicities on f_{cov} . A log-normal distribution of metallicities around the mean $\log(Z_{\text{DLA}}/Z_{\odot}) = -1.0$ with a standard deviation of $\sigma_{\log(Z_{\text{DLA}}/Z_{\odot})} = 0.5$ was assumed, with lower/upper limits to $\log(Z_{\text{DLA}}/Z_{\odot}) = -4.0/0.0$ respectively. This upper and lower limit to the metallicity reflects the range of metallicities observed in DLAs (Prochaska et al. 2003). In this model $\lesssim 8\%$ of the DLAs have metallicities $\log(Z_{\text{DLA}}/Z_{\odot}) > -0.5$ and < -1.5 . The covering factor is increased more by the high metallicity DLAs than it is reduced by the low metallicity systems (this trend can be seen in Figure 2). As a result, the scatter causes a net small increase in f_{cov} ; in the range $\tau_{0.5} = 0.1 - 0.2$ we find the increase in f_{cov} to be $\lesssim 25\%$, which is most likely well within model uncertainties mentioned above.

The redshift of the source, z_s , has only a small effect on the results for $\tau_{0.5} \gtrsim 0.1$. The reason is that with the $f(N_{\text{HI}}, z)$ adopted from P03, the absorption is dominated by low redshift systems; e.g. 75% of the contribution to f_{cov} comes from $z < 0.61$. The contribution from sources with $z \gtrsim 1.4$ is practically negligible. This inference, however, depends sensitively on the poorly known redshift–evolution of $f(N_{\text{HI}}, z)$; which is discussed in more detail in §4.2.

The main conclusion from Figure 2 is that for a source similar to 4C41.17, which has size of ~ 100 arcsec², observed at \sim arcsec resolution, one can hope to find several pixels covered by DLAs with opacities up to $\tau_{0.5} \sim 0.1 - 0.2$. Of course, for a source covering a larger solid angle and/or in the case of an unusually enriched DLA, there is significant probability of finding more opaque absorption. For example, in the case of an X-ray emitting galaxy cluster with ~ 10 times the area of 4C41.17 (see below), the figure shows that DLAs with $\tau \gtrsim 0.3$ should typically obscure several pixels.

3. OBSERVABILITY

The ideal background source would be a bright and perfectly smooth extended X-ray source. In this idealized case a foreground DLA (or that part of the DLA that lies in front of the extended X-ray source) shows up in absorption against the background source in the very soft X-ray band (0.3–0.6 keV). In practice, extended X-ray sources are not smooth, but have surface brightness fluctuations that are much larger than the $\sim 10\%$ level introduced by absorption due to intervening DLAs. For example, the fluctuations in the number of X-ray photons received from different locations in 4C41.17 exceeds $\sim 100\%$. The main reason for this is small number statistics. The mean number of counts per pixel is \sim a few, and therefore Poisson noise will make variations between individual pixels large. In 3C294 (Fabian et al. 2003), the mean number of counts per pixel is higher by a factor of a few and therefore Poisson noise is less severe, although still large enough to introduce errors well in excess of 10%. Large holes in the X-ray map of 3C294 are clearly seen, from which no X-rays at all are detected, and which are too large to arise from an intervening absorber. They probably arise from intrinsic spatial variations in the population of relativistic particles responsible for the scattering.

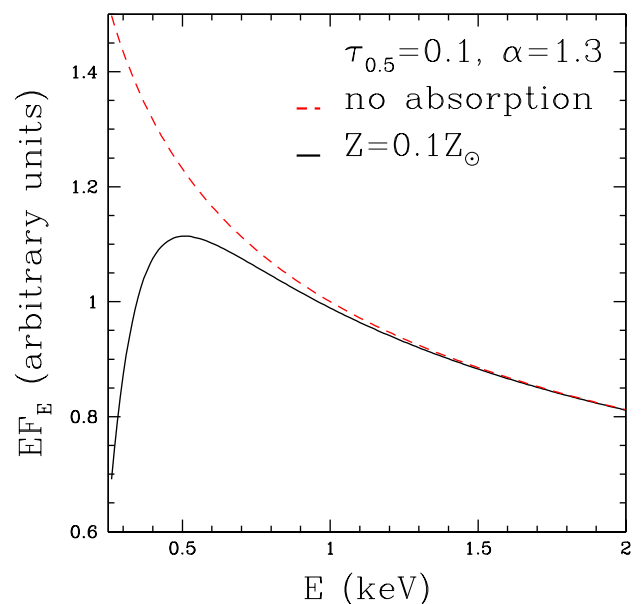


FIG. 3.— Power law spectrum, $F_E \propto E^{-1.3}$ of an unobscured (*dashed curve*), and an obscured (*solid curve*) X-ray source. The latter spectrum assumes that the source is obscured by an intervening DLA with an optical depth $\tau_{0.5} = 0.1$. In Figure 1 the corresponding column for $Z_{\text{DLA}} = 0.1Z_{\odot}$ can be read off as a function of z .

We next describe two methods to distinguish the intrinsic surface brightness fluctuations from those caused by absorption.

3.1. Spectral Imprints of DLAs

Because the absorption cross section is a strong function of energy ($\sigma_{\text{tot}} \propto E^{-3}$), the spectrum of an attenuated portion of the extended X-ray source can, in principle, reveal whether X-rays have been absorbed by an intervening column of gas. In order to make a crude estimate of the sensitivity of X-ray observations to DLA attenuation, we here quantify the absorption signature in a simple toy-model. In reality, an X-ray observatory has a potentially complex, energy dependent, detection efficiency, which must be taken into account in a more detailed analysis

(see further discussion below).

In Figure 3, we show the spectrum of an attenuated patch of a power-law source in the 0.25-2.0 keV range, in which absorption has removed 10% of the 0.5 keV photons, alongside the spectrum of an unattenuated patch. The background source has a spectrum $F_E \propto E^{-\alpha}$ with $\alpha = 1.3$ (motivated by the inverse Compton spectrum observed in 4C41.17). The units of the flux are arbitrary. Clearly, the spectra are most distinct at energies $E \lesssim 0.6$ keV. To quantify the difference, we introduce the ratio \mathcal{R} , which is the ratio of the number of photons received in the very soft (0.3-0.6 keV) and the soft (0.6-2.0 keV) band. In Figure 4, we plot \mathcal{R} in the case of no absorption for a power law $F_E \propto E^{-\alpha}$ spectrum as a function of α together with \mathcal{R} for cases in which $\tau_{0.5} = 0.05, 0.1$ and 0.2 .

Figure 4 shows, for example, that if the intrinsic X-ray spectrum is given by $F_E \propto E^{-1.3}$, then $\mathcal{R} = 1.9$ in the case of no absorption, but \mathcal{R} decreases to ≤ 1.2 for $\tau_{0.5} \geq 0.2$. There is, of course, a degeneracy with α , and \mathcal{R} can also equal ≤ 1.2 with no absorption but $\alpha \leq 0.8$. Two approaches to lift this degeneracy are: (i) α can be determined and extrapolated from the $E \gtrsim 1.0$ keV part of the spectrum, and/or (ii) computing \mathcal{R} as a function of position may reveal areas where \mathcal{R} is significantly lower than in the rest of the source. The latter approach is similar to mapping out dust using an optical map, with the difference that obscured parts of the X-ray source look 'bluer', rather than redder.

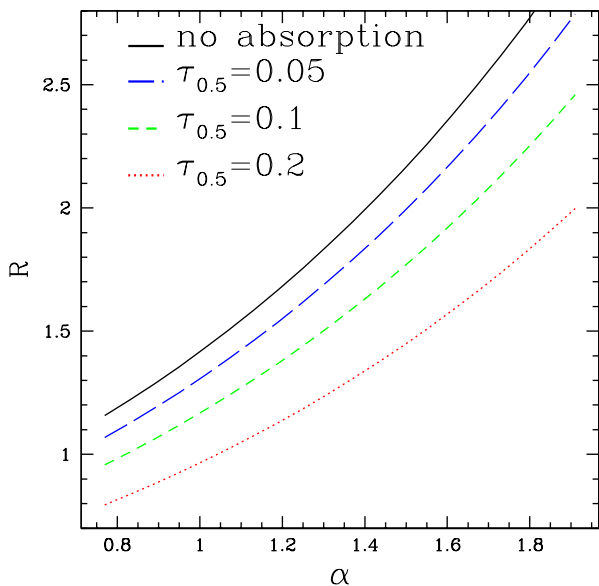


FIG. 4.— The ratio of the number of photons in the observed 0.3-0.6 keV and 0.6-2.0 keV bands, defined as \mathcal{R} , as a function of the slope of the spectrum α . The different curves correspond to different amounts of absorption for a range of 0.5 keV optical depths of 0–0.2, as shown by the labels.

3.1.1. Photon Statistics

We next address the uncertainty in α and \mathcal{R} , as determined by the number of photons from a given location. Assuming that we receive n_{ph} photons from a location in the energy range 0.3-8.0 keV, the number of photons for $\alpha = 1.3$ in the 0.3-0.6, 0.6-2.0, 2.0-8.0 keV bands is $60(n_{\text{ph}}/100)$, $33(n_{\text{ph}}/100)$ and $7(n_{\text{ph}}/100)$, respectively. When the spectrum in the 0.6-2.0 and 2.0-8.0 keV bands is binned to two data points from which we extract the slope of the spectrum α , and assuming Pois-

son noise in the number of photons, the error² in α is $\sigma_{\alpha} \approx 0.3(n_{\text{ph}}/100)^{-0.5}(\alpha/1.3)^{2.0}$. The $\alpha^{2.0}$ dependence of the error reflects the fact that when α is larger, there are fewer photons in the hard band, making the uncertainty in the number of photons there larger. The error in \mathcal{R} can be similarly computed and is similar, $\sigma_{\mathcal{R}} = 0.25\mathcal{R}(n_{\text{phot}}/100)^{-0.5}$.

From Figure 4, we find that with ~ 100 photons in the 0.3-8.0 keV band, we can distinguish between $\tau_{0.5} = 0.2/0.1$ (which predict $\mathcal{R} = 1.2$ and 1.5 , respectively) and the no-absorption case (which predicts $\mathcal{R} = 1.9$) at the $\sim 2 \times (\alpha/1.3)^{-2}\sigma$ and $\sim 1 \times (\alpha/1.3)^{-2}\sigma$ level, respectively.

The above estimates ignore the processing of the input signal through the X-ray instrument. The instrumental response should have little effect on the *relative reduction* in the number of photons, but a low overall detection efficiency can reduce the signal-to-noise. The typical response function of X-ray telescopes like *Chandra* are strong functions of energy. *Chandra* is a factor of $\sim 1.5-2/3-4$ more sensitive at $E = 1.0$ keV than it is at $E = 0.5/0.3$ keV. The number of photons in the 0.3-0.6 keV band will therefore be less by a factor of $\lesssim 3$ than expected for a pure powerlaw. Therefore the error on \mathcal{R} will be larger by a factor of $\lesssim \sqrt{3}$, which implies we need $\gtrsim 300$ photons in the 0.3-8.0 keV band, to distinguish between $\tau_{0.5} = 0.2/0.1$ and $\tau_{0.5}$ at the $\sim 2 \times (\alpha/1.3)^{-2}\sigma$ and $\sim 1 \times (\alpha/1.3)^{-2}\sigma$ level, respectively.

3.1.2. Influence of Galactic HI

The analysis so far has concentrated on distinguishing between absorption and no-absorption cases. In practise the no-absorption case is hypothetical, since Galactic HI will cause additional absorption. In 4.1 we discuss observations showing that Galactic HI in a typical extragalactic line of sight will not vary across angular scales comparable to the sizes of known extended X-ray sources. Therefore, instead of distinguishing between $\tau_{0.5} = 0$ and $\tau_{0.5} = 0.1/0.2$, we need to distinguish between $\tau_{0.5} = \tau_{\text{Gal}} \sim 0.1$ and $\tau_{0.5} = 0.1/0.2 + \tau_{\text{Gal}}$. The value $\tau_{\text{Gal}} \sim 0.1$ is typical for the galaxy, although there are large parts of the sky in which it is less than that by a factor of a few (see §4.1). The particular value of τ_{Gal} along the line of sight to a given X-ray source can be ascertained accurately in a follow-up radio observation. A low value of τ_{Gal} is preferred, although it will not make much difference for DLAs with $\tau_{0.5} = 0.1$, since the difference between $\tau_{0.5} = 0$ and 0.1 is comparable to that between $\tau_{0.5} = 0.1$ and 0.2 (see Figure 4).

3.1.3. Required Integration Times on Chandra

Ideally, we need surface brightness maps with arcsec resolution to be able to differentiate between compact clumps ($d \lesssim 5$ kpc) and large disks ($R \gtrsim 15$ kpc, or $D \gtrsim 30$ kpc.), since 1 arcsec corresponds to $\sim 7-8.5$ kpc in the redshift range 0.7-4.0. To reduce telescope time, the maps can be binned to a resolution of 2×2 arcsec². If the DLA gas resides in a large ($D \gtrsim 30$ kpc) disk, it will then still be resolved in over $\gtrsim 4$ resolution elements.

To obtain $\gtrsim 3 \times 10^2$ photons per resolution element, we need $\gtrsim 75$ per arcsec². For comparison, 4C41.17 observed for 100 ksec on *Chandra* by Scharf et al. (2003) only has a few photons per arcsec² over its ~ 100 arcsec² area.

Another source, 3C294, was observed for 200 ksec with *Chandra* and has $\sim 4-6$ photons per arcsec² over most of its area of

²This formula is an approximation for the error obtained when standard error analysis is applied. The approximation is valid in the range $0.5 \leq \alpha \leq 2.2$.

~ 200 arcsec² (Fabian et al. 2003). This suggests that in order to obtain $\gtrsim 75$ photons per arcsec², we need approximately 3 Msec of integration by *Chandra* for a source similar to 4C41.17 and 3C294. Grego et al. (2004) observed a distant ($z = 0.8$) galaxy cluster for 100 ksec using *Chandra*. In their observation an area as large as $\sim 10^3$ arcsec² had more than 2.5 photons per arcsec², suggesting that again a 3 Msec observation would give enough photons to look for absorption in this area. The origin of the X-rays in this case is mainly thermal, and the analysis given above for a power-law inverse Compton spectrum does not apply. However, a cluster X-ray spectrum in reality is more complex, with many heavy element emission lines superimposed on a multi-temperature thermal Bremsstrahlung spectrum (Raymond & Smith 1977). A power law with photon index of $\alpha \approx 0.5 - 1$ can be therefore used as a simple first order approximation, and similar statistics will apply.

In practice, for any source, one would proceed by first determining the mean *observed* spectrum of the entire extended X-ray source. This mean spectrum can then be used as a template, to seek differential spectral deviations in spatial bins along the surface of the source. An advantage of using galaxy clusters (over the X-ray halos of radio galaxies) is their potentially larger angular size, which allows a search for the rarer DLAs with more significant opacity.

3.2. Combining X-ray and Sunyaev-Zeldovich Effect Maps

Another way to determine whether a dimming of certain part(s) in the X-ray image is due to absorption or due to an intrinsic brightness fluctuation in the source itself is to map the CMB temperature decrement, caused by the Sunyaev-Zeldovich (SZ) effect, along the surface of the source. This decrement should scale with the intrinsic X-ray brightness, regardless of whether the origin of the X-rays is thermal or non-thermal. In particular, thermal X-ray emission scales with the line-of-sight integral of n_e^2 , whereas inverse Compton emission and the SZ surface brightness both scale with the line of sight integral of n_e (where n_e is the electron number density). Local density variations can therefore cause thermal X-ray/SZ brightness variations. However, the thermal X-ray flux is unlikely to drop noticeably without an accompanying decrease in the SZ decrement. In contrast, an intervening DLA would not have any effect on the SZ decrement. An SZ map with \sim arcsec resolution will therefore be very useful in constraining the intrinsic X-ray brightness fluctuations. This resolution is feasible with future mm-telescopes, such as ALMA³. Whether ALMA is sensitive enough to detect SZ temperature decrements due to sources like 4C41.17 can be estimated as follows: As a first order estimate, the temperature decrement at $\nu \sim 100 - 200$ GHz can be approximated by $\Delta T_{\text{CMB}} \sim (N_e T_e / 10^{28} \text{ K cm}^{-2}) \mu\text{K}$, where N_e is the column density of electrons in the X-ray source, $T_e = \bar{E}/k$ is the electron temperature, and \bar{E} is the mean electron energy. The product $N_e T_e$ is directly proportional to the observed rate of X-ray photons, \dot{N}_γ , which is given by $\dot{N}_\gamma = \epsilon dV / (4\pi d_L^2(z) d\Omega \bar{E}_\gamma)$ photons/cm²/sec/sr. Here $\epsilon = 5.4 \times 10^{-36} T_e N_e (1+z)^4$ ergs/sec/cm³ is the volume emissivity from inverse Compton emission (e.g., Katz et al. 1996); $d_L(z)$ is the luminosity distance; \bar{E}_γ is the mean observed photon energy, and $dV/d\Omega$ are differential volume/solid angle elements. For 4C41.17, ~ 2 photons per arcsec² are observed, implying $N_e T_e \sim 10^{30}$ in the above units. Therefore, we find $\Delta T_{\text{CMB}} \sim 10^2 \mu\text{K}$, which can be detected by ALMA in a several-hour integration (Kocsis et al. 2004).

³<http://www.alma.nrao.edu/>

4. DISCUSSION

4.1. Is the Absorption Arising in a DLA?

We described in §2 what fraction of the area of a diffuse X-ray source is covered by DLAs with columns high enough to block out an observable fraction of the X-rays. In §3 we showed how we can distinguish this attenuation by a DLA from intrinsic brightness fluctuations in the source itself. Our method, however, does not constrain the redshift of the absorber. When a positive detection of absorption by a foreground column of, say, $N_{\text{HI}} = 10^{21} \text{ cm}^{-2}$ is made, there is a possibility that the hydrogen gas is physically associated with the source. Whether significant amount of neutral hydrogen can co-exist with the hot, X-ray emitting gas should depend primarily on the local cooling efficiency. In recent work, Birnboim & Dekel (2003) and Keres et al. (2004) have argued that significant neutral gas is present only around low-mass, high-redshift galaxies. Sources that are sufficiently X-ray bright to allow the detection of a DLA are likely to be associated with more massive objects (such as powerful radio galaxies), in which the local neutral hydrogen would be absent.

Nevertheless, a disadvantage of using X-rays is that the absorption contains no redshift information (unless lines are detected, but this requires many more photons), so there is no immediate way to rule out the local-absorption hypothesis observationally. In any case, absorption in a region that is several arcsec across would imply the neutral hydrogen gas associated with the source itself would extend several tens of kpc across, which would be an interesting alternative interpretation of any future detection. The DLA or local absorption hypotheses can be distinguished by optical follow-up observations: in general, there will be no bright background quasar dominating the optical images, and associated faint galaxies will be easier to identify than in the case of DLAs discovered in optical quasar spectra.

Similarly, the absorption can take place in a local ($z \sim 0$) hydrogen cloud. The column of hydrogen required for $\tau_{0.5} = 0.1$ is $\gtrsim 3 \times 10^{20} \text{ cm}^{-2}$ for metallicities less than $0.1 Z_\odot$. These columns are reached typically in cold disks of late-type galaxies in the nearby universe, which would be bright and easy to identify in optical images. Alternatively, a nearby, low-mass compact HI cloud, with no Galactic counterpart, is almost certainly ruled out. Absorption by an nearby HI cloud with $\log(N_{\text{HI}}/\text{cm}^{-2}) = 21$ requires an HI mass of $4 \times 10^5 (d/10 \text{ Mpc})^2 (\theta/5'')^2 M_\odot$ compressed in a cloud of radius $0.125 (d/10 \text{ Mpc}) (\theta/5'')$ kpc. Here, θ is the angular size of the absorption feature measured in arcsec, and d the distance to the HI cloud measured in Mpc. This implies a mean number density of $\sim 0.3 (d/10 \text{ Mpc})^{-1} (\theta/5'')^{-1} \text{ cm}^{-3}$ and these clouds would most likely rapidly cool and collapse on a dynamical timescale, which is $\sim 1/\sqrt{G\rho} \sim 10^8$ yrs.

Although Galactic HI is present in large columns, it is unlikely to present a problem beyond a reduction of the overall signal-to-noise discussed above. The average column of hydrogen within our own galaxy is $\langle N_{\text{HI}} \sin|b| \rangle = 3 \times 10^{20} \text{ cm}^2$, where b is Galactic latitude and $\langle \dots \rangle$ denotes the average over an annulus at b Lockman e.g., 2003. Assuming a solar abundance pattern of $Z = 0.7 Z_\odot$ (which is the appropriate value for the ISM, e.g. Wilms et al. 2000) for this column, this translates to $\langle \tau_{\text{Gal}} \sin|b| \rangle = 0.1$. Because of spatial variations of Galactic N_{HI} , there are large portions of the sky where τ_{Gal} is lower by a factor of a few. These spatial variations occur predominantly

on large ($> 1^\circ$) angular scales, and therefore τ_{Gal} can be considered as a constant over the entire X-ray source. The r.m.s. spatial fractional variation in Galactic N_{HI} is $< 3\%$ on angular scales $< 1^\circ$, with larger fluctuations occurring on smaller angular scales only in directions of anomalously high galactic N_{HI} (Lockman 2003).

4.2. The Uncertainties in $f(N_{\text{HI}}, z)$

The total number of DLAs used by P03 to constrain $f(N_{\text{HI}}, z)$ in the DLA range of N_{HI} was 114. This data was binned in 4 redshifts bins covering the redshift ranges $z = 0.0-2.0$, $2.0-2.7$, $2.7-3.5$ and $z > 3.5$ each containing between 23 and 49 DLAs. P03 fitted a Schechter function, $f(N_{\text{HI}}, z) = (f_*/N_*) (N_{\text{HI}}/N_*)^{-\beta} \exp(-N_{\text{HI}}/N_*)$, to the data in each bin. Prochaska & Herbert-Fort (2004) identified six new DLAs at $z > 3.5$ in an automated search for DLAs in the quasar spectra of Data Release 1 of the Sloan Digital Sky Survey (SDSS), and found that including these six new DLAs changed the fitting parameters (f_* , N_* , β) of P03 significantly at $z > 3.5$ which they attribute to the small sample size in this bin⁴. For the same reason the obtained values for the fitting parameters in the lowest redshift bin are uncertain.

Not only the fitting parameters, the fitting function itself is uncertain. Using a Schechter function to describe $f(N_{\text{HI}}, z)$ introduces a sharp cutoff at high N_{HI} . P03's $f(N_{\text{HI}}, z)$ provides a good fit to the column density distribution over most of the z and N_{HI} range. However, at the high- N_{HI} regime that is relevant for our purposes, other functional forms (with less sharp cut-offs in N_{HI}) can provide equally good fits.

We therefore find that the largest uncertainties in $f(N_{\text{HI}}, z)$ are in regions of (N_{HI}, z) -space that are most relevant for our purposes. As can be seen in Figure 1, the column required to produce $\tau_{0.5} = 0.1$ increases rapidly with redshift ($\propto (1+z)^3$). As the high column systems are rare, the largest contribution to f_{cov} in the P03 model comes from low redshift. However, the increase in the number of DLAs with redshift is uncertain, and could compensate the increase in $N_{\text{HI}, \text{min}}$.

In summary, our estimate of f_{cov} is uncertain, but is likely to be conservative, since P03 may have underestimated the number of high N_{HI} , especially at higher redshift.

4.3. Mapping out Known DLAs

So far we have focused on examining an extended X-ray source and searching for evidence of an intervening DLA. As mentioned before, several hundred known DLA are observed in the redshift range $z = 0.1-4.6$. A complementary approach may be to look for extended X-ray sources behind these known DLAs. The Scharf et al. (2003) source was chosen for X-ray study because it was an example of a cluster of sub-mm sources, centered on a powerful radio galaxy, and was therefore considered a probable proto-galaxy-cluster with X-ray emission. Extended X-ray sources at high redshifts may indeed turn out to be common, especially around radio-loud galaxies. Of the several hundred known DLAs in front of quasars, $\sim 10\%$ will be along sight-lines to radio loud quasars. A certain fraction of these radio loud quasars will be similar to the 4C41.17 source. This fraction is unknown at present, but is unlikely to be negligible. A similar source observed behind a known DLA is Q1354+258. This source appears to have an extended structure in the radio, and also is known to have a diffuse Lyman

⁴These authors also note that P03 has obtained systematically too low values of N_{HI} for $\log(N_{\text{HI}}/\text{cm}^{-2}) > 21$.

α blob around it, similar to 4C41.17. This DLA is located at $z = 2.0$, and it has a column of $3.2 \times 10^{21} \text{ cm}^{-2}$, but a rather low metallicity $Z \sim 10^{-2} Z_\odot$, translating to a value of $\tau_{0.5} = 0.09$. Nevertheless, this suggests that a systematic search for DLAs whose parent quasar is similar to 4C41.17, and deep X-ray observations of these sources, is a promising alternative approach to discover X-ray silhouettes of DLAs.

5. CONCLUSIONS

The neutral hydrogen column densities in observed DLAs are in the range $\log(N_{\text{HI}}/\text{cm}^{-2}) = 20-21.7$ (e.g. Curran et al. 2002) and are high enough to absorb a measurable fraction of soft X-ray photons from a background source. We defined the parameter $\tau_{0.5}$, which is the optical depth through DLAs for a photon with an observed energy of 0.5 keV. We found that $\sim 1\%$ of the sky is covered by DLAs which have $\tau_{0.5} \geq 0.2$ when the background X-ray sources lie at redshifts greater than $z \gtrsim 1.4$. This result depends on the assumed column density distribution $f(N_{\text{HI}}, z)$, which is at present poorly constrained, and also on the mean metallicity of the DLAs, which we assumed to be $Z = 0.1 Z_\odot$. This corresponds to the mean observed metallicities in DLAs (e.g. Prochaska et al. 2003). Although the scatter between individual objects is large, we find that it does not significantly increase the covering factor.

An optical depth of $\tau_{0.5} = 0.2$ will introduce dimming by $\sim 18\%$ only, by an amount that is much lower than intrinsic brightness fluctuations. However, as we discussed in §3, absorption by an intervening DLA can be distinguished from intrinsic brightness fluctuations by looking for the spectral signatures of absorption (see Figure 3) and/or combining the X-ray observations with an SZ decrement map of the area (§3.2).

We showed that in order to reliably distinguish between absorption and no-absorption, $\lesssim 2$ arcsec resolution, and $\gtrsim 300$ photons per angular resolution element are required in the 0.3–8 keV band. For diffuse, high redshift X-ray sources similar to 4C41.17 (Scharf et al. 2003) and 3C294 (Fabian et al. 2003), this requires observation times of a few Msec on *Chandra*. Although challenging, this is likely to be the only viable method to directly spatially resolve hydrogen gas in DLAs in the foreseeable future. Among planned future radio telescopes, only SKA is able to detect 21cm emission from neutral hydrogen at $z > 0.5$ (e.g., van der Hulst et al. 2004).

The planned X-ray observatories *XEUS* (Parmar 2003) and *Generation X* (Zhang et al. 2002) are expected to have $\sim 1-0.1$ arcsec resolution, and a sensitivity of one or two orders of magnitude better than *Chandra*, extending to energies as low as 0.1 keV. At these low energies, absorption by a foreground DLA will leave a much stronger imprint. The X-ray silhouettes of DLAs should be feasible to detect in routine observations with these planned instruments.

We thank Joop Schaye, Jason Prochaska and Art Wolfe for useful comments. ZH gratefully acknowledges support by the National Science Foundation through grants AST-0307291 and AST-0307200 and by NASA through grant HST-GO-09793.18.CS acknowledges the support of NASA/Chandra grant SAO G03-4158A.

REFERENCES

- Bagla, J. S. 1999, in ASP Conf. Ser. 156: Highly Redshifted Radio Lines, 9–15
 Bahcall, J. N., & Peebles, P. J. E. 1969, ApJ, 156, L7+
 Bechtold, J., Siemiginowska, A., Aldcroft, T. L., Elvis, M., & Dobrzycki, A. 2001, ApJ, 562, 133

- Birnboim, Y., & Dekel, A. 2003, MNRAS, 345, 349
- Briggs, F. H., Wolfe, A. M., Liszt, H. S., Davis, M. M., & Turner, K. L. 1989, ApJ, 341, 650
- Chen, H., & Lanzetta, K. M. 2003, ApJ, 597, 706
- Clarke, T. E., Uson, J. M., Sarazin, C. L., & Blanton, E. L. 2004, ApJ, 601, 798
- Curran, S. J., Webb, J. K., Murphy, M. T., Bandiera, R., Corbelli, E., & Flambaum, V. V. 2002, Publications of the Astronomical Society of Australia, 19, 455
- Fabian, A. C., Sanders, J. S., Crawford, C. S., & Etori, S. 2003, MNRAS, 341, 729
- Grego, L., Vrtilek, J. M., Van Speybroeck, L., David, L. P., Forman, W., Carlstrom, J. E., Reese, E. D., & Joy, M. K. 2004, ApJ, 608, 731
- Haehnelt, M. G., Steinmetz, M., & Rauch, M. 1998, ApJ, 495, 647
- Kanekar, N., & Briggs, F. H. 2003, A&A, 412, L29
- Katz, N., Weinberg, D. H., & Hernquist, L. 1996, ApJS, 105, 19
- Keres, D., Katz, N., Weinberg, D. H., & Dave, R. 2004, MNRAS, submitted
- Kocsis, B., Haiman, Z., & Frei, Z. 2004, ApJ, submitted, astro-ph/0409430
- Lockman, F. J. 2003, in Soft X-ray Emission from Clusters of Galaxies and Related Phenomena, astro-ph/0311386, ed. R. Lieu & J. Mittaz
- Parmar, A. N. e. a. 2003, in X-Ray and Gamma-Ray Telescopes and Instruments for Astronomy. Edited by Joachim E. Truemper, Harvey D. Tananbaum. Proceedings of the SPIE, Volume 4851., 304–313
- Prochaska, J. X., Gawiser, E., Wolfe, A. M., Castro, S., & Djorgovski, S. G. 2003, ApJ, 595, L9
- Prochaska, J. X., & Herbert-Fort, S. 2004, PASP, 116, 622
- Prochaska, J. X., & Wolfe, A. M. 1997, ApJ, 487, 73
- Rao, S. M., Nestor, D. B., Turnshek, D. A., Lane, W. M., Monier, E. M., & Bergeron, J. 2003, ApJ, 595, 94
- Rao, S. M., & Turnshek, D. A. 2000, ApJS, 130, 1
- Raymond, J. C., & Smith, B. W. 1977, ApJS, 35, 419
- Scharf, C., Smail, I., Ivison, R., Bower, R., van Breugel, W., & Reuland, M. 2003, ApJ, 596, 105
- Spergel, D. N. e. a. 2003, ApJS, 148, 175
- Storrie-Lombardi, L. J., & Wolfe, A. M. 2000, ApJ, 543, 552
- van der Hulst, J. M., Sadler, E. M., Jackson, C. A., Hunt, L. K., Verheijen, J. H., & van Gorkom, J. H. 2004, in Science with the Square Kilometer Array, ed. C. Carilli & S. Rawlings (Elsevier Science Publishers)
- Wilms, J., Allen, A., & McCray, R. 2000, ApJ, 542, 914
- Wolfe, A. M., Lanzetta, K. M., Foltz, C. B., & Chaffee, F. H. 1995, ApJ, 454, 698
- Zhang, W., Petre, R., & White, N. 2002, in COSPAR, Plenary Meeting